

Optimization of 3D turbo GluCEST MRI of healthy brain at 7T

Kejia Cai^{1,2}, Hari Hariharan¹, Anup Singh¹, Mohammad Haris^{1,3}, Kevin D'Aquilla¹, Ravi Prakash Reddy Nanga¹, Feliks Kogan¹, and Ravinder Reddy¹
¹Radiology, University of Pennsylvania, Philadelphia, PA, United States, ²CMRR 3T Research Program, Radiology, University of Illinois at Chicago, Illinois, IL, United States, ³Sidra Medical and Research Center, Doha, Qatar, United States

Target audience: Basic science and clinical scientists who are interested in research on neuroimaging and brain function.

Introduction/Purpose: Glutamate (Glu) is the primary neurotransmitter responsible for excitatory synaptic transmission in the central nervous system. Excessive Glu in the synaptic space can trigger a toxic cascade leading to neuronal death, which has been implicated in a wide range of neurological and psychiatric disorders¹. GluCEST, an imaging technique that utilizes the chemical exchange saturation effect of Glu has been exploited for mapping Glu in brain¹ and spinal cord² at the ultra-high field 7T. Also, single slice high-resolution GluCEST map has been produced to image the spatial distributions of Glu in subcortical brain structures³. However, the distribution of neurological lesions may not be fully accessible from a single slice 2D GluCEST map that limit its application and 3D GluCEST mapping is necessary to localize Glu abnormalities in a large brain volume. The purpose of this study is to extend the 2D GluCEST for 3D imaging. A turbo acquisition method has been investigated and optimized for scan time efficiency.

Methods: Under an approved Institutional Review Board (IRB) protocol, all experiments were performed on a Siemens 7T whole-body scanner with a vendor supplied 32-channel volume RF coil. GluCEST MRI was performed in a group of healthy male subjects (n=5, 24-63 years old). The 3D GluCEST MRI of 8 or 16 brain slices was performed using a new custom built 3D version of the previous sequence¹. The saturation Hanning-windowed pulse train (total 750 ms, 99.8% duty cycle, B_1 rms of 155 Hz or 3.6 μ T) was followed by Fast Low-Angle SHot imaging (FLASH) centric multi-partition k-space readout (flip angle = 5°, readout TR/TE = 6.3/3 ms). A variable number of partitions (slice encodes) are acquired in a single shot. The other default imaging parameters are: number of averages = 1, slice thickness = 5 mm, field of view = 200 × 200 mm², matrix size = 192 × 192, shot TR = 15 s, flip angle = 5 degree, number of dummy scans = 4, number of partitions = 4. Raw CEST images with varying saturation offsets were acquired from ±2.3 to ±3.7 ppm (relative to water resonance) with a 0.35 ppm increment. A total of 10 measurements were acquired. To remove field inhomogeneities induced artifacts in GluCEST maps, images for B_1 and ΔB_0 field mapping were acquired and used for GluCEST reconstruction as previously described¹⁻⁴. To optimize the imaging parameters, flip angle and the number of dummy scans were varied from 3° to 10° and from 4 to 64 respectively to acquire the 3D saturation “off” images. The signal to noise ratio (SNR) and the ghost to noise ratio (GNR) were quantified based on manually drawn regions of interest. The SNR was calculated as the signal from the entire brain divided by the standard deviation of white noise. The GNR was calculated as the signal from a noise region with ghost-artifact divided by the standard deviation of white noise. Number of partitions was varied from 1 to 8 for 3D GluCEST imaging and the CEST contrast maps were generated accordingly. Image processing and data analysis was performed using MATLAB (version 7.5, R2007b).

Results: With increased flip angle, brain SNR and GNR increase as demonstrated in Figure 1A-B. Ghost effect increases the artifact noise level mainly along the phase encoding direction and blurs the brain image. To balance the SNR and GNR, 5° is chosen as the optimized value. It is close to the Ernst angle (4.9°) when TR is 6 ms and T_1 is 1.6 s. Figure 1C-D shows that with number of dummy scans of 4 or more, SNR and GNR are kept relatively constant with only slight reduction. However, large number of dummy scans may delay the acquisition of the central k-space data and reduces the CEST image contrast. Hence, small number of dummy scans such as 4 or 8 is considered to be optimal. In case of the centric acquisition, the high spatial frequencies of k space are acquired towards the end of the reading when signal is reduced due to spin dephasing. As a result, acquisition with large number of partitions prolongs the reading time and causes blurring in the fine structures of brain. As shown in Figure 1F-I, gray and white matter regions are more and more separated as the number of partition increases due to the loss of visibility of fine structures. The CEST contrast ratio of overall gray matter over white matter increased from 1.44 ± 0.06 , 1.47 ± 0.02 , 1.50 ± 0.01 to 1.71 ± 0.02 as the number of partitions increased from 1, 2, 4 to 8. However, the acquisition time reduces proportionally to the number of partition. To balance the acquisition time and the integrity of the signal from fine structures, the number of partition 4 may be used. With the experimentally optimized parameters (5° flip angle, 4 dummy scans and 4 partitions), Figure 2 shows a set of 3D GluCEST maps of 16 slices with the first and the last slices removed due to fold over artifacts. The 3D GluCEST acquisition time is 10 min. To avoid the fold over, phase oversampling may be used.

Discussion: This initial study demonstrates that 3D GluCEST MRI is feasible. Further studies to develop isotropic voxel 3D GluCEST imaging by incorporating parallel imaging and key-hole imaging techniques are under investigation.

Funding: This project was supported by the National Institute of Biomedical Imaging and Bioengineering of the National Institutes of Health through Grant Number P41-EB015893 and P41-EB015893S1. **References:** [1] Cai, K. et al. *Nature Medicine*. 2012; 18(2): 302-6. [2] Kogan, F. *Neuroimage*. 2013; 77:262-7. [3] Cai, K. et al. *NMR Biomed*. 2013;26:1278-1284. [4] Singh, A. et al. *MRM*. 2012; 69(3):818-824.

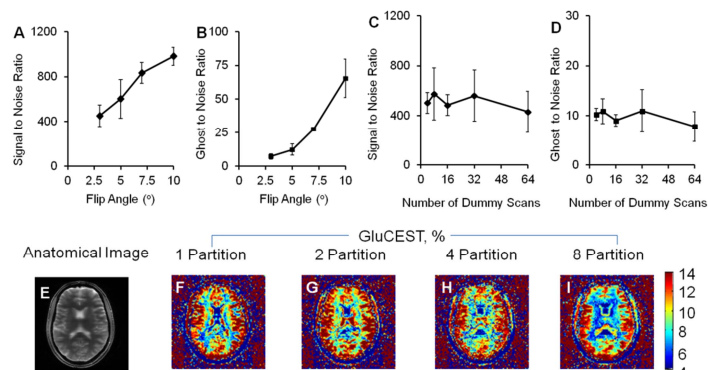


Figure 1. SNR and GNR dependence on flip angle (A-B) and the number of dummy scan (C-D). GluCEST maps (F-I) reconstructed from CEST images acquired with different partitions, 1 to 8 from left to right.

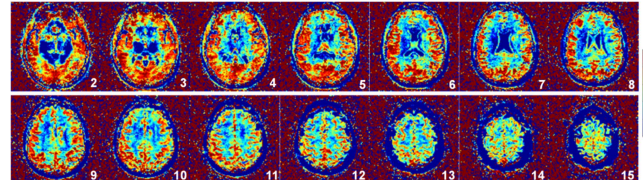


Figure 2. A representative 3D acquisition of 16 GluCEST maps acquired under experimentally optimized parameters. The first and the last slices are removed due to the fold over artifacts.